Noticeable Reverse Shift in the Melting Temperatures of Benzene and Carbon Tetrachloride Confined within the Micropores and Mesopores of Hydrophobic Carbons

Katsumi Kaneko, Fitri Khoerunnisa, Daiki Minami, Ryusuke Futamura, Ayumi Watanabe, Yohko Hanzawa and Takaomi Suzuki

Noticeable Reverse Shift in the Melting Temperatures of Benzene and Carbon Tetrachloride Confined within the Micropores and Mesopores of Hydrophobic Carbons[†]

Katsumi Kaneko[1,*], Fitri Khoerunnisa[1], Daiki Minami[1], Ryusuke Futamura[1], Ayumi Watanabe[2], Yohko Hanzawa[3] and Takaomi Suzuki[4] *(1) Research Center for Exotic Nanocarbons, Shinshu University, Nagano 380-8553, Japan. (2) Material Science, Department of Chemistry, Graduate School of Science and Technology, Chiba University, Chiba 263-8522 Japan. (3) Faculty of Engineering, Chiba Institute of Technology, Narashino, Chiba 275-0023, Japan. (4) Faculty of Engineering, Shinshu University, Nagano 380-8553, Japan.*

ABSTRACT: Carbon aerogels contain both mesopores and micropores. In this study, benzene/CCl_4 was adsorbed in the pores of carbon aerogels (both mesopores and micropores) and their phase behaviours were examined using differential scanning calorimetry. The bulk solid benzene melted at 278 K and the melting temperatures of benzene confined inside the mesopores and micropores of carbon aerogels were 258 and 293 K, respectively. Although the melting temperature depression of condensates in mesopores is well known, the observed elevation of the melting temperature for micropores is very limited in the strongly interacted system. Similar melting behaviours were observed for the confined CCl_4; depression by 45 K in mesopores and elevation by 48 K in micropores showed about two times the change as compared with that of confined benzene.

INTRODUCTION

Porous materials have played an important role in nature and modern technology. Fluids are adsorbed in pores and the condensates in pores induce phase transition such as melting or freezing, which is associated with biological and geological activities. IUPAC have classified pores into micropores (w < 2 nm), mesopores (2 nm < w < 50 nm) and macropores (w > 50 nm) (Sing *et al*. 1985). It is well known that vapour condensates in mesopores below the saturated vapour pressure, and melting or freezing temperature of the condensates is depressed according to the Gibbs–Thomson equation (Jackson and Mc Kenna 1990; Mu and Malhotra 1991; Unruh *et al*. 1993; Defay *et al*. 1996). Because it is quite difficult to determine the correct freezing temperature due to serious supercooling, the fusion process has been studied to a greater extent than freezing. The low temperature shift of the melting temperature has been used for evaluating the mesopore size (Quinson *et al*. 1986). Therefore, the freezing of condensates in mesopores has been studied with reference to capillary condensation for a long time. Branton *et al*. (1994, 1996) showed unusual condensation behaviour in regular mesoporous silica whose pore width is less than approximately 5 nm, stimulating the experimental and molecular simulation studies (Ravikovitch *et al*. 1995; Inoue *et al*. 1998; Sarkisov and Monson 2001; Kruk and Jaroniec 2002; Ravikovitch and Neimark 2002; Kowalczyk *et al*. 2006; Thommes *et al*. 2006, 2012; Morishige 2008).

Adsorption mechanism in typical micropores, the so-called micropore filling, is markedly different from capillary condensation due to overlapping of the molecule–pore wall interactions (Everett and Powl 1976), as elucidated by Sing and Gregg [Gregg and Sing (1982); Sing (1989)]. The micropore filling has given rise to the active studies using molecular simulation (Balbuena and Gubbins 1992; Lastoskie *et al*. 1993; Pikunic *et al*. 2005). Molecules adsorbed in the micropores cannot be regarded as the liquid phase. It was shown evidently that water and ethanol confined in hydrophobic micropores of graphitic micropore walls form a solid-like structure even at 303 K (Iiyama *et al*. 1995; Ohkubo *et al*. 1999) and also other molecules or atoms in the micropores have a unique structure different from the bulk liquid or solid (Kaneko *et al*. 1995; Kaneko 1996; Urita *et al*. 2011; Kaneko *et al*. 2012; Khoerunnisa *et al*. 2012). Very recently, molecular rotation of methane molecules adsorbed in the tube spaces of single-wall carbon nanohorn is quenched even above the bulk boiling temperature, suggesting the elevation of the boiling temperature of adsorbed methane (Hashimoto *et al*. 2011). Therefore, we have a quite fundamental question: Whether molecular assemblies in micropores can be regarded as a phase and whether they can behave in a similar way to condensates in mesopores or macroscopic liquid or solid. Miyahara and Gubbins predicted that the freezing temperature of fluids confined in micropores and small mesopores should be elevated in case of a strong interaction of the molecule with the pore wall (Miyahara and Gubbins 1997). In a previous work, we experimentally showed the elevation of benzene and CCl_4 adsorbed onto activated carbon fibres (Kaneko *et al*. 1999; Watanabe *et al*. 1999). In addition, Sliwinska-Bartkowiak *et al*. introduced impedance measurement to exhibit the elevation of fluids confined in micropores (Sliwinska-Bartkowiak *et al*. 1999, 2008; Sliwinska-Bartkowiak and Jazdzewska 2010; Lung *et al*. 2011).

In this study, we examined the phase behaviours of benzene and CCl_4 confined in graphitic micropores and mesopores of carbon aerogels, by assuming that condensates confined in both pores should behave differently.

EXPERIMENTAL SECTION

Synthetic carbon aerogels were used as the graphitic pore systems having both micropores and mesopores (Pekala *et al*. 1992; Hanzawa *et al*. 1998, 2002). The microporosity and mesoporosity were determined by high-resolution N_2 adsorption isotherm at 77 K using the subtracting pore effect method (Kaneko *et al*. 1992) for high resolution α_s plot (Table 1). The α_s plot analysis was introduced by Sing *et al*. and is used to understand the mechanism of micropore filling in porous carbons (Atkinson *et al*. 1984; Sing *et al*. 1985; Sing 1989; Kenny *et al*. 1993). The subtracting pore effect method of the α_s plot can accurately evaluate the surface area of carbon-slit pores whose width is larger than 0.7 nm (Setoyama *et al*. 1998).

Benzene or CCl_4 was adsorbed at 303 K under the saturated vapour pressure after drying carbon aerogels at 373 K for 2 hours. The carbon samples with adsorbed fluids were sealed in the aluminium pan. The differential scanning calorimetric (DSC) chart was recorded at a scanning rate temperature of 5 K·min^{-1} using the DSC system (DSC-3100; MAC Science). The melting temperature was determined by the crossing point of the linear dropping part of the peak and the average background. The enthalpy of melting was obtained from the peak area. The freezing temperature was also determined using the rising linear part of the peak. Tables 2 and 3 show the melting temperature and enthalpy of fusion, respectively, for confined benzene and CCl_4 in carbon aerogel.

TABLE 1. Porosity of Carbon Aerogel by Nitrogen Adsorption

	Specific surface area (m^2 g^{-1})	Pore volume (cm^3 g^{-1})	Average pore width (nm)
Micropores	370	0.11	0.63
Mesopores	350	1.19	13.6

TABLE 2. Melting Temperature for Confined Benzene and CCl$_4$ in Carbon Aerogel

		Melting temperature (K)	Transition
Benzene	Bulk	278	Solid to liquid
In mesopore	258		
In micropore	292		
CCl4	Bulk	223	Monoclinic to rhombohedral solid
		243	Rhombohedral solid to liquid
	In mesopore	203	Monoclinic to rhombohedral solid
		220	Rhombohedral solid to liquid
	In micropore	296	Solid to liquid

Table 3. Enthalpy of Fusion for Confined Benzene and CCl$_4$ in Carbon Aerogel

	Enthalpy of fusion (kJ mol^{-1})	
	Benzene	CCl$_4$
Bulk	10.42	1.57
In mesopores	4.94	0.589
In micropores	0.457	1.01×10^{-2}

RESULTS AND DISCUSSION

Figure 1 shows DSC curves of benzene confined in the pores of carbon aerogels and the bulk one. The observed melting temperature of bulk solid benzene is 278 K, which is in agreement with the value reported in the literature (Watanabe *et al.* 1999). The freezing temperature of bulk benzene was observed to be approximately 255 K, which is lower than the melting temperature due to the marked supercooling. One can observe a distinct endothermic peak at 265 K on the heating curve of confined benzene. The corresponding exothermic peak can be observed at 238 K on the cooling curve. These peaks, which are distant from those of the bulk benzene, are ascribed to melting and freezing of benzene adsorbed in mesopores. The melting temperature of benzene adsorbed in mesopores was 258 K, which is slightly different from the peak temperature. Thus, a remarkable depression (20 K) of melting temperature is observed for benzene confined in mesopores. The shift of the melting temperature calculated using the Gibbs–Thomson equation is 32 K, which is approximately close to the observed one. A careful examination provides a small melting peak at 294 K and the corresponding freezing peak is observed at 292 K, as shown in Figure 2. These should be attributed to melting and freezing of benzene adsorbed in micropores, based on a previous work about freezing temperature shift of benzene adsorbed in micropores; in the
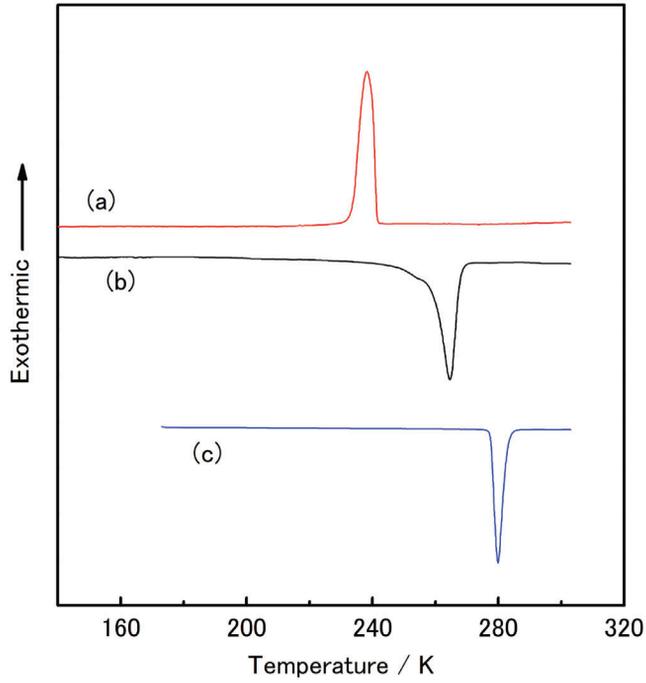
Figure 1. DSC heating and cooling curves of benzene adsorbed on carbon aerogel. The DSC heating curve of bulk benzene is shown for comparison: (a) cooling and (b) heating of adsorbed benzene; (c) heating of bulk benzene.
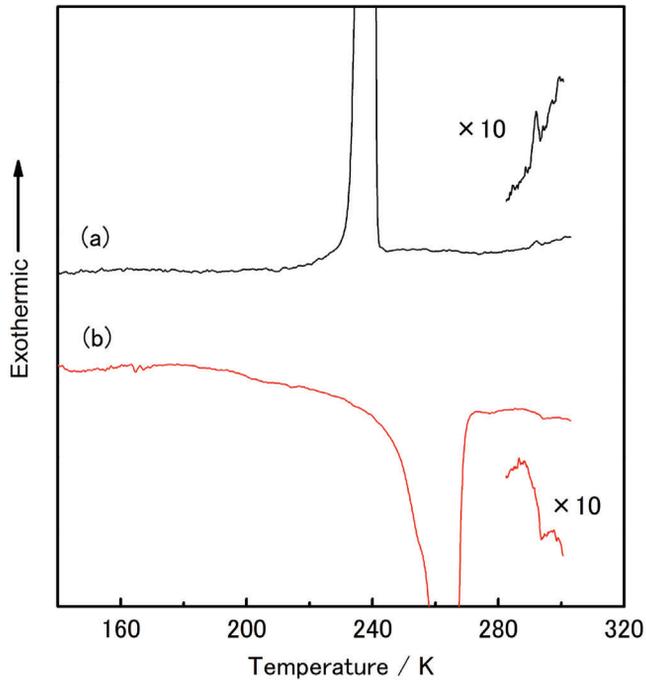
Figure 2. Magnified DSC curves of benzene adsorbed on carbon aerogel: (a) cooling and (b) heating.

preceding works (Kaneko *et al*. 1999; Watanabe *et al*. 1999), we showed that the meaningful peak could be deduced by averaging several DSC charts. The melting temperature of the benzene confined in micropores is 293 K, and is elevated by 15 K. The elevation of the freezing temperature is also observed.

Figure 3 shows the heating curves of confined and bulk CCl_4. The heating curve of bulk solid CCl_4 has two peaks at 223 and 248 K, which originate from the monoclinic to rhombohedral solid-phase transition and the rhombohedral solid to liquid-phase transition at 223 and 248 K, respectively (Koga and Morrison 1975; Morrison and Richard 1976). The observed phase transition temperatures are closed to those in reported in the literature. These phase transition temperatures of CCl_4 confined in mesopores are 203 and 220 K, which are lower than those of the bulk one by more than 28 K. Not only the melting temperature, but also the solid-phase transition temperature is depressed by confinement in mesopores. The Gibbs–Thomson equation provided a depression of 52 K using the bulk surface tension value. There is a small endothermic peak at 297 K, which stems from the melting of CCl_4 adsorbed in micropores, giving the melting temperature of 296 K. Thus, the elevation of the melting temperature is 48 K. The melting temperature of benzene and CCl_4 confined in micropores is remarkably elevated, while the melting temperature is depressed for those condensates in mesopores. This study using carbon aerogels of uniform micropores and mesopores explicitly shows the completely different phase behaviours of fluids confined in micropores and mesopores.
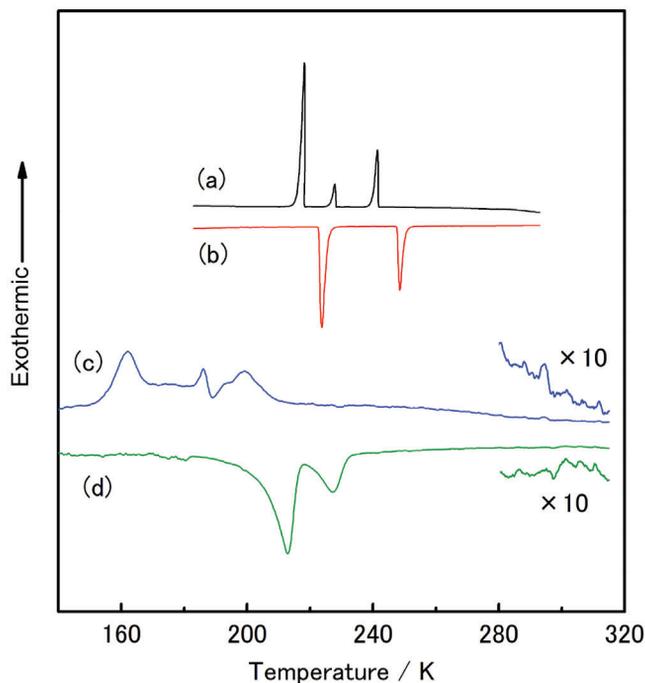
Figure 3. DSC curves of CCl_4 adsorbed on carbon aerogel and bulk CCl_4: (a) cooling of bulk CCl_4; (b) heating of adsorbed CCl_4; (c) cooling; (d) heating.

The observed small enthalpy of fusion for fluids confined in micropores should come from the highly organized structure of liquid and solid phases of fluids confined in graphitic micropores. The inter-molecular structure of fluids in the micropores is different from that of bulk one, as already mentioned earlier. The liquid state of confined benzene is partially ordered, while the solid state is disordered due to a serious geometrical restriction for the formation of a well-crystalline solid structure. Consequently, the enthalpy difference between partially ordered liquid and imperfect solid states of confined fluids is quite small, as observed here.

A molecular simulation study by Miyahara and Gubbins (1997) suggested that when the interaction potential energy of a molecule with the pore wall is greater than that with the solid surface made of the adsorbate molecules, the freezing (or melting) temperature shifts to a higher side with a decrease in pore width, which reduces the melting process of micropores by molecular simulation. The calculated interaction potential of benzene and CCl_4 molecule with the graphitic slit pore of w = 0.63 nm is 50 and 60 kJ mol^{-1}, respectively. These calculated interaction potentials are much greater than the enthalpy of sublimation. Hence, these systems satisfy the conditions predicted by Miyahara and Gubbins. The system giving a greater interaction potential leads to a more pronounced elevation of the melting temperature, and thereby the high temperature shift of the melting temperature of CCl_4 is greater than that of benzene.

Our study results explicitly indicate that the phase behaviour of confined fluids depends sensitively on the pore size, and the phase transition temperature of fluids in mesopores and micropores dramatically shifts to a completely opposite direction.

ACKNOWLEDGEMENTS

REFERENCES

Atkinson, D., Mc Lead, A.I., Sing and K.S.W. (1984) *J. Chem. Phys.* **81**, 791.

Balbuena, P.B. and Gubbins, K.E. (1992) *Fluid Phase Equilib.* **76**, 721.

Branton, P.J., Hall, P.G., Sing, K.S.W., Reichert, H., Schüth, F. and Unger, K. (1994) *J. Chem. Soc., Faraday Trans.* **90**, 2965.

Branton, P.J., Kaneko, K., Setoyama, N., Sing, K.S.W., Inagaki, S. and Fukushima, Y. (1996) *Langmuir* **12**, 599.

Defay, R., Prigogine, I., Belleman, A. and Everett, D.H. (1966) Effect of curvature on the equilibrium state of a pure substance. In: *Surface Tension and Adsorption*, Longmans, London.

Everett, E. H. and Powl, J. C. (1976) *J. Chem. Soc. Faraday Trans.* **72**, 619.

Gregg, S.J. and Sing, K.S.W. (1982) *Adsorption , Surface Area and Porosity*, Academic Press, London.

Hanzawa, Y., Hatori, H., Yoshizawa, N. and Yamada, Y. (2002) *Carbon* **40**, 4, 575.

Hanzawa, Y., Kaneko, K., Yoshizawa, N., Pekala, R.W. and Dresselhaus, M.S. (1998) *Adsorption* **4**, 187.

Hashimoto, S., Fujimori, T., Tanaka, H, Urita, K., Ohba, T., Kanoh, H., Itoh, T., Asai, M., Sakamoto, H., Niimura, S., Endo, M., Rodoriguez-Reinoso, F. and Kaneko, K. (2011) *J. Am. Chem. Soc.* **133**, 2022.

Iiyama, T., Nishikawa, K., Otowa, T. and Kaneko, K. (1995) *J. Phys. Chem.* **99**, 10075.

Inoue, S., Hanzawa, Y. and Kaneko, K. (1998) *Langmuir* **14**, 3079.

Jackson, C.L. and Mc Kenna, G.B. (1990) *J. Chem. Phys*. **93**, 9002.

Kaneko, K. (1996) *Colloids Surf*. **109**, 319.

Kaneko, K., Iiyama, T., Wang, Z. and Hanzawa, Y. (1995) *Adv. Porous Mater*. 401.

Kaneko, K., Ishii, C., Ruike, M. and Kuwabara, H. (1992) *Carbon* **30**, 1075.

Kaneko, K., Itoh, T. and Fujimori, T. (2012) *Chem. Lett*. **41**, 466.

Kaneko, K., Watanabe, A., Iiyama, T. and Radhakrishnan, R. (1999) *J. Phys. Chem. B* **103**, 7061.

Kenny, M.B., Sing, K.S.W. and Theocharis, C.R. (1993) *Fundamentals of Adsorption*, Kodansha and Elsevier Science, Tokyo and Amsterdam.

Khoerunnisa, F., Fujimori, T., Itoh, T., Urita, K., Hayashi, T., Kanoh, H., Ohba, T., Hong, S.Y., Choi, Y.C., Santosa, S.J., Endo, M. and Kaneko, K. (2012) *J. Phys. Chem. C* **116**, 11216.

Koga, Y. and Morrison, J.A. (1975) *J. Chem. Phys*. **62**, 3359.

Kowalczyk, P., Kaneko, K., Solarz, L., Terzyk, A.P., Tanaka, H. and Hołyst, R. (2006), *Langmuir* **21**, 6613.

Kruk, M. and Jaroniec, M. (2002) *J. Phys. Chem. B* **106**, 4732.

Lastoskie, C., Gubbins, K. E. and Quirke, N. (1993), *J. Phys. Chem*. **97**, 4786.

Lung, Y., Palmer, J.C., Coasne, B., Sliwinska-Bartkowiak, M. and Gubbins. K.E. (2011) *Phys. Chem. Chem. Phys*. **13**, 17163.

Miyahara, M. and Gubbins, K.E. (1997) *J. Phys. Chem*. **106,** 2865.

Morishige, K. (2008) *Adsorption* **14**, 157.

Morrison, J.A. and Richards, E.L. (1976) *J. Chem. Thermodyn*. **8**, 1033.

Mu, R. and Malhotra, V.M. (1991) *Phys. Rev*. **48B**, 9021.

Ohkubo, T., Iiyama, T., Nishikawa, K., Suzuki, T. and Kaneko, K. (1999) *J. Phys. Chem*. **103**, 1859.

Pekala, R.W., Alviso, C.T., Kong, F.M. and Hulsey, S.S. (1992) *J. Non-Cryst. Solids* **145**, 90.

Pikunic, J., Llewellyn, P., Pellenq, R. and Gubbins, K.E. (2005) *Langmuir* **21**, 4431.

Quinson, J.F., Dumas, J. and Serughetti, J. (1986) *J. Non-Cryst. Solids* **79**, 397.

Ravikovitch, P.I., Domhanail, S.C.O., Neimark, A.V., Schuth, F. and Unger, K.K. (1995) *Langmuir* **3**, 443.

Ravikovitch, P.I. and Neimark, A.V. (2002) *Langmuir* **18**, 9830.

Sarkisov, L. and Monson, P.A. (2001) *Langmuir* **17**, 7600.

Setoyama, N., Suzuki, T. and Kaneko, K. (1998) *Carbon* **36**, 1459.

Sing, K.S.W. (1989) *Carbon* **27**, 5.

Sing, K.S.W., Everett, D.H., Haul, R.A.W., Moscou, L., Rerotti, R.A., Rouquerol, J. and Seimieniewska, T. (1985) *Pure Appl. Chem*. **57**, 603.

Sliwinska-Bartkowiak, M., Gras, J., Sikorski, R., Radhakrishan, R., Gelb. L. and Gubbins, K.E (1999) *Langmuir* **15**, 6060.

Sliwinska-Bartkowiak, M. and Jazdzewska, M. (2010) *J. Chem. Eng. Data* **55**, 4183.

Sliwinska-Bartkowiak, M., Jazdzewska, M., Huang, L.L. and Gubbins, K.E. (2008) *Phys. Chem. Chem. Phys*. **10**, 4909.

Thommes, M., Cychosz, K.A. and Neimark, A.V. (2012) Advanced physical adsorption characterization of nanoporous carbons. In: *Novel Carbon Adsorbents*, J.M.D. Tascon, editor. Elsevier, Amsterdam, p. 107.

Thommes, M., Smarsly, B., Groenewolt, M., Ravikovitch, P.I. and Neimark, A.V. (2006) *Langmuir* **22**, 756.

Unruh, K.M., Huber, T.E. and Huber, C.A. (1993) *Phys. Rev*. **48B**, 9021.

Urita, K., Shiga, Y., Fujimori, T., Iiyama, T., Hattori, Y., Kanoh, H., Ohba, T., Tanaka, H., Yudasaka, M., Iijima, S., Moriguchi, I., Okino, F., Endo, M. and Kaneko, K. (2011) *J. Am. Chem. Soc*. **133**, 27, 10344.

Watanabe, A., Iiyama, T. and Kaneko, K. (1999) *Chem. Phys. Lett*. **305**, 71.